

## MORPHOLOGICAL DETAILS OF STRAIN-INDUCED MARTENSITE IN COLD-ROLLED Cr – Ni STEEL

Agnieszka Kurc-Lisiecka

WSB University in Poznan, Faculty of WSB University in Chorzow, Institute of Applied Sciences, Department of Logistics and Management Engineering, 29 Sportowa Str., 41-506 Chorzow, Poland

Corresponding author: Agnieszka Kurc-Lisiecka, [agnieszka.kurc-lisiecka@chorzow.wsb.pl](mailto:agnieszka.kurc-lisiecka@chorzow.wsb.pl)

**Abstract:** The investigation presents the evolution of strain-induced martensite during cold rolling of AISI 304 stainless steel at 10% and 50% degree of deformation. The morphologies and characteristics of  $\alpha'$  martensite have been studied using optical-image analysis, scanning and transmission electron microscope. The influence of strain-induced martensite on mechanical properties and hardness of AISI 304 steel have been reported.

Plastic deformation during the cold rolling of AISI 304 steel induces a martensitic transformation ( $\gamma \rightarrow \alpha'$ ) in the whole range of applied deformation degree. The equiaxial grains of austenite containing annealing twins were observed within the microstructure of steel at delivery state. During the deformation process the shape of austenite grains was changed into long slim bands parallel to the rolling direction. Many shear bands and micro-twins were observed in the microstructure at large deformations degrees. The martensite, which was formed as a result of the transformation ( $\gamma \rightarrow \alpha'$ ) induced by deformation, has a distinct influence on properties of the investigated steel grade. It was found that the effect of steel hardening is a result of a significant increase of the volume fraction of the  $\alpha'$ -martensite in the structure.

**Key words:** austenitic stainless steels, cold rolling, microstructure, phase transformation, strain-induced martensite.

### 1. INTRODUCTION

The stainless steels are very attractive industrial materials in terms of their superior corrosion resistance, appearance and mechanical properties. They are widely used in food, chemical, machinery, automobile and nuclear industry. However, some of these austenitic steels with a lower content of Ni are unstable upon deformation (for example cold rolling). As a result, the austenite phase is transformed into martensite in these steels. Such martensitic transformation during plastic deformation imparts a good combination of strength and toughness to austenitic stainless steels. In general, the martensitic transformation is considered to be induced when an austenitic

stainless steel is deformed at temperatures below  $M_d$ , a temperature below which the transformation to martensite readily occurs (Das, 2008). In addition to the  $M_d$  temperature, martensitic transformation is believed to be affected by several other factors such as: chemistry, strain rate, strain, stress state and temperature of deformation (Lo et al., 2009). Mechanical stability of austenite in Cr-Ni steels and their susceptibility to martensitic transformation and  $\alpha'$  phase formation is determined in literature (Padilha and Rios 2002, Ahlers 2004, Dai et. al. 2004, Hedström 2007), indirectly, by  $M_s$  and  $M_d$  temperature values.

In the case of austenitic steels, the  $M_s$  temperature is determined from various relationships given respectively by Bavay (Bavay, 1993), Eichelman and Hull (Eichelman and Hull, 1998, as cited in Padilha et. al., 2003) and Andrews (Andrews, 1965, as cited in Das et. al., 2008). The Equation 1 formulated by gives an approximation the temperature of  $\alpha'$  martensite formation ( $M_s$ ). This temperature is strongly connected with the chemical composition of the alloy and for all austenitic stainless steels series 300, it can be calculated by the formula:

$$M_s(^{\circ}\text{C}) = 502 - 810(\% \text{ C}) - 1230(\% \text{ N}) - 13(\% \text{ Mn}) - 30(\% \text{ Ni}) - 12(\% \text{ Cr}) - 54(\% \text{ Cu}) - 6(\% \text{ Mo}) \quad (1)$$

In Cr-Ni steels, with a relatively low proportion of alloying additives (mainly Ni), the martensitic transformation can occur partially at room temperature (Fig.1).

Higher contents of these additives provide higher austenite stability and a lower  $M_s$  temperature, well below room temperature (Bavay, 1993).

The  $M_s$  temperature of selected Cr-Ni austenitic steels is relatively low and in some cases reaches values close to  $-200^{\circ}\text{C}$  (Bavay, 1993). However, the low value of this temperature does not exclude martensitic transformation during typical cooling of these steels.

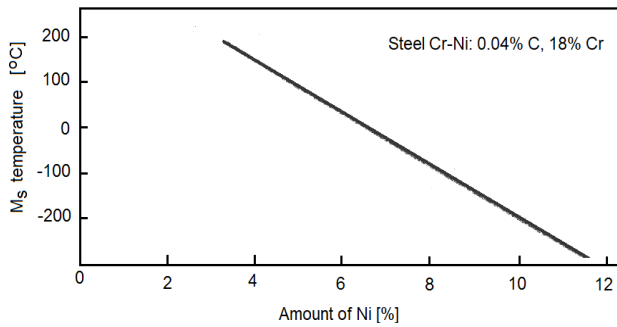


Fig.1. Dependence of  $M_s$  temperature on Ni content in Cr-Ni steel [5]

This is due to the separation of  $M_{23}C_6$  carbide at the austenite grain boundary resulting in a decrease in Cr and C content in the boundary zone. As a consequence, the  $M_s$  temperature locally increases, which allows the transformation to proceed and martensite to form  $\alpha'$ . Mechanical stability of austenite indirectly determined by the  $M_s$  temperature, which in turn is determined by the free energy, i.e. the chemical composition of the  $\gamma$  phase, as well as its fragmentation, may alternatively be determined by other parameters related to this energy but derived from the stress and strain state of the material. The temperature values  $M_{s\sigma}$  and  $M_d$  are a measure of this stability of austenite (Fig.2.)

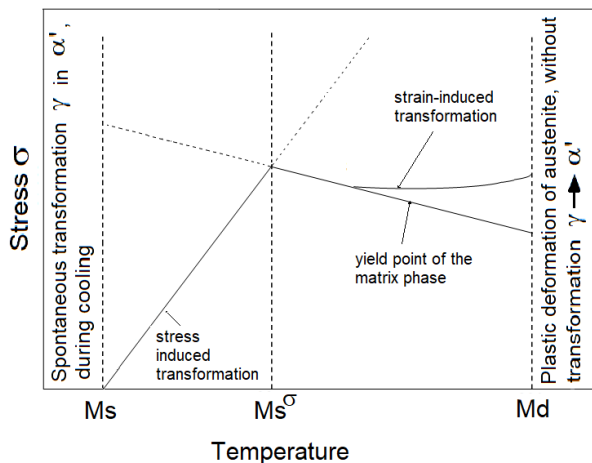


Fig.2. The dependence of occurrence of martensitic transformation on temperature  $M_s$ ,  $M_{s\sigma}$  and  $M_d$  as well as the stress and strain state of steel [22]

In steel cooled below the  $M_s$  temperature, a typical martensitic transformation occurs in which martensite forms on pre-existing nucleation sites. However, above the  $M_s$  temperature, a stress-induced martensitic transformation occurs on the same nuclei in a certain  $M_s$ - $M_{s\sigma}$  temperature range. The transformation of austenite into the so-called "strain" martensite occurs at increasing values of stress with increasing temperature, reaching at  $M_{s\sigma}$  temperature the value at which the applied stress inducing martensitic transformation is equal to the yield strength of the matrix phase. Plastic deformation above  $M_{s\sigma}$  temperature implies a different mechanism of

martensitic transformation, in which the nucleation sites of so-called martensite "deformation" may be specific dislocation groups, in areas of plastic deformation. Near the  $M_{s\sigma}$  temperature, the transformation of austenite to martensite is activated by both mechanisms. On the other hand, the  $M_d$  temperature is the maximum temperature above which no deformation leads to a martensitic transformation (Shin et al., 2001; Dai et al., 2004).

In order to determine the start temperature of the martensitic transformation induced by cold plastic deformation ( $M_d$ ), the empirical relations (2) and (3) were also used, determining the so-called  $M_{d30}$  temperature, according to Bavay (Bavay, 1993) as well as Angel (Angel, 1954), respectively.

$$M_{d30}(^{\circ}\text{C}) = 497 - 13.7(\% \text{ Cr}) - 20(\% \text{ Ni}) - 8.1(\% \text{ Mn}) - 18.5(\% \text{ Mo}) - 9.2(\% \text{ Si}) - 462(\% [\text{C} + \text{N}]) \quad (2)$$

$$M_{d30}(^{\circ}\text{C}) = 413 - 13.7(\% \text{ Cr}) - 9.5(\% \text{ Ni}) - 8.1(\% \text{ Mn}) - 18.5(\% \text{ Mo}) - 9.2(\% \text{ Si}) - 462(\% [\text{C} + \text{N}]) \quad (3)$$

The  $M_{d30}$  is a temperature at which, in steel plastically deformed with a 30% of deformation, the 50% of martensite is formed.

Relationships (2) and (3) consider the same weight percent of carbon and nitrogen in the steel, although they were developed for stainless steels with nitrogen contents lower than typically found in these steels. They can be used for austenitic steels containing up to a maximum of about 9% Mn. Since the stability of austenite depends on the N and Ni contents, the

quotient of the weight ratios  $\left( \frac{x \cdot (\% \text{ N})}{y \cdot (\% \text{ Ni})} \right)$  was

determined for relations (2) and (3). For relation (2), the determined quotient of the weighting ratios of N and Ni is ca. 23, and for relation (3) it is ca. 48. This means that in low-nickel steels, in which the expensive nickel is replaced by nitrogen, high N content ensures obtaining, as a result of annealing, homogeneous austenitic structure with lower susceptibility to martensite formation during cold plastic deformation, in comparison with classical austenitic Cr-Ni. Bavay (Bavay, 1993) also found, based on relation (2), that an increase in nickel content in steel inhibits the formation of plastic deformation-induced martensite  $\alpha'$  in its structure, while Ti stabilization has the opposite effect by decreasing the C and N contents in the solid solution.

During plastic deformation of A1 lattice (fcc) metals and alloys, a microstructure is formed that depends mainly on the stacking fault energy (SFE) value, chemical composition, strain temperature, and thermodynamic phase stability. The fcc energy of austenitic stainless steel can be determined from the chemical composition from the empirical relation (4)

given by Schramm and Reed (Schramm and Reed, 1975) such as:

$$\text{SFE (mJ/m}^2\text{)} = -53 + 6.2(\% \text{Ni}) + 0.7(\% \text{Cr}) + 3.2(\% \text{Mn}) + 9.3 (\% \text{Mo}) \quad (4)$$

According to relation (4), in which the effect of C and N is not considered, elements such as Ni, Mo, Mn, and Cr determine the increase in SFE. On the other hand, according to the relation proposed by Bavay (Bavay, 1993), Ni and C increase SFE, while Cr, N, Si, and Mn decrease it.

The metastability of austenite stainless steels increases with the decrease of SFE (Reed, 1962; Schramm and Reed, 1975).

In the work (Leber et al., 2004), the effect of chemical composition on SFE value and martensite  $\alpha'$  and  $\epsilon$  formation in 304L, 316L, 321, 347 grade austenitic steels was studied after deformation in the range from 10% to 60%. The investigated steels are characterized by high phase  $\gamma$  stability as evidenced by SFE values in the range of 25 to 30 mJ/m<sup>2</sup>. The SFE values calculated according to relations (4).

It has been found that in steels with high SFE (>30 mJ/m<sup>2</sup>) and a typical slip system (111)[1-10], martensite  $\alpha'$  can be formed alternatively, either directly from austenite or with the participation of an intermediate hexagonal  $\epsilon$  phase. In contrast, in steels with low SFE (<30 mJ/m<sup>2</sup>), the slip system (111)[-12-1] occurs during the phase transformation, which favors the formation of martensite  $\epsilon$ .

Many studies have been devoted to the phase transformation of metastable austenite into martensite  $\alpha'$  in austenitic Cr-Ni steels (Amar et al., 2004; Shrinivas et al., 1995). Generally, it is assumed that the hexagonal phase  $\epsilon$  is an intermediate phase between austenite and martensite  $\alpha'$  with the transformation sequence  $\gamma \rightarrow \epsilon \rightarrow \alpha'$  (Cina, 1958). Both the formation of martensite  $\epsilon$  and its presence in the intermediate stage of the phase transformation,  $\gamma \rightarrow \alpha'$  depends on the SFE value (Venables, 1962; Lagneborg, 1964). Its low value is conducive to the formation of the hexagonal phase, while with a higher SFE value, austenite can either be transformed directly into martensite  $\alpha'$ , or undergo a transformation through the hexagonal phase  $\epsilon$ . However, it takes place very quickly, and therefore it is relatively difficult to determine its presence (Lagneborg, 1964).

The presence of strain-induced martensite can be a detrimental phenomenon and can cause delayed cracking of deep-drawn austenitic stainless steel components. On the other hand, martensite formation due to plastic deformation of metastable austenite is of great interest for the production of high-strength and ductile austenitic stainless steels (Kurc-Lisiecka et al., 2016).

Although the martensitic transformation in metastable austenitic steels has been studied by many authors, the

understanding developed for a particular alloy system under certain deformation conditions cannot be generalised to other metastable systems. Therefore, research is needed to understand the strain-induced phase transformation in specific cases. Accordingly, the aim of the present study was to analyze morphological details of strain-induced martensite in cold-rolled 304 AISI steel.

## 2. MATERIAL AND EXPERIMENTAL PROCEDURE

The experiments were conducted on AISI 304 stainless steel containing 0.024 pct C, 18.53 pct Cr, 7.8 pct Ni, 1.32 pct Mn, 0.43 pct Si, 0.028 pct P, 0.005 pct S, 0.01 pct Ti, 0.01 Al S by weight. Material for investigation was provided from UGINE&ALZ (Poland) in the form of steel strip, 2 mm thick, 40 mm in width and 700 mm long was supersaturated in water after its austenitizing for 1 hour at a temperature of 1100°C. After supersaturation the AISI 304 stainless steel plates were processed by unidirectional cold rolling, impressing 10, 20, 30, 40 and 50 pct reductions in thickness. Plastic deformation of the steels studied was carried out in the process of cold rolling on a Skoda QUATRO type 10502 mill with 430 mm roll diameter, using a peripheral speed of rolls equal to 0.65 m/s (Fig.3). The scheme of the longitudinal rolling process of the tested AISI 304 steel have been presented in Table 1.

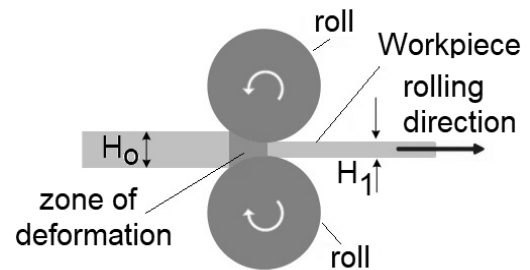


Fig.3. Cold longitudinal rolling process of the tested AISI 304 steel; roll diameter 430 mm, roll peripheral speed 0.65 m/s

Rolling was carried out at 20°C using small unit crumples, keeping the direction and side of the rolled strip constant. The degree of deformation during the rolling process was determined alternatively, assuming no sheet expansion, based on relations (5) and (6), (Pater, 2014):

$$Z_H = \frac{H_0 - H_1}{H_0} \cdot 100\% \quad (5)$$

$$\epsilon_H = \ln \frac{H_0}{H_1} \quad (6)$$

where:

$z_H$  – degree of deformation (draft), [%]

$H_0$  - thickness of sheet before deformation, [mm]

$H_1$  - thickness of sheet after deformation, [mm]

$\varepsilon_H$  - logarithmic deformation.

The individual sheet band passes were characterized by additionally giving the magnitude of the total deformation,  $Z_S$ .

Based on the chemical composition of the investigated steel the  $M_s$ ,  $M_{d30}$  and SFE were calculated (Table 2). The mechanical properties of investigated steel were determined applying static tensile test and measurements of the hardness. The static tensile tests

were carried out on the universal strength machine ZWICK 100N5A at RT (room temperature) at a strain rate of  $10^{-3}s^{-1}$  and included cold rolled samples. Standard 20-mm wide tensile test specimens according to PN-EN ISO 6892-1, cut from the AISI 304 steel sheet along the rolling direction were used for measurements of the mechanical properties.

The hardness measurements of the analyzed AISI 304 steel were carried out by a hardness tester FM 700 produced by Future-Tech (Japan), according to the standard PN-EN ISO 6507-1. Researches were made by Vickers's method on metallographic samples with a load of 50N and a measurement time of 30 s.

Table 1. Schematic of the longitudinal rolling process for the tested AISI 304 steel

No.	Number of the culvert												Deformation		
	0	1	2	3	4	5	6	7	8	9	10	11			
	Sheet thickness [mm]												Z <sub>H</sub> [%]	Z <sub>S</sub> [%]	ε <sub>H</sub>
1	2.0	–	–	–	–	–	–	–	–	–	–	–	–	–	–
2	2.0	1.85	1.8	–	–	–	–	–	–	–	–	–	10	10.2	0.10
3	2.0	1.85	1.8	1.7	1.65	1.6	–	–	–	–	–	–	20	21.7	0.22
4	2.0	1.85	1.8	1.7	1.65	1.6	1.5	1.4	–	–	–	–	30	34.6	0.35
5	2.0	1.85	1.8	1.7	1.65	1.6	1.5	1.4	1.25	1.2	–	–	40	49.3	0.51
6	2.0	1.85	1.8	1.7	1.65	1.6	1.5	1.4	1.25	1.2	1.05	1.0	50	66.6	0.69

Table 2. Calculated values of SFE and temperature of martensitic transformation for investigated AISI 304 steel

SFE (mJ/m <sup>2</sup> )	Temperature of martensitic transformation (°C)	
	$M_s$	$M_{d30}$
12.55	9.04	60.3

The microstructure investigations were performed by using a optical-image analysis, scanning and transmission electron microscopy.

Metallographic observations using a light microscope were made on longitudinal and transverse samples of the examined AISI 304 steel sheets in the as delivered condition, after supersaturation and after cold rolling.

Peparation of the specimens for testing included mechanical grinding and polishing and etching procedures. The samples for microstructure observation were etched in Mi17Fe reagent containing according to ASTM E407: 10cm<sup>3</sup> nitric acid HNO<sub>3</sub>, 100cm<sup>3</sup> hydrochloric acid HCl and 90cm<sup>3</sup> distilled water heated to 40°C. The etched of the samples was carried out at a time ranging from 20 s to 120 s. Metallographic studies were carried out using an OLYMPUS GX71 (Japan)

light microscope equipped with an electronic record of observation documentation at magnifications from 100 to 2000x.

The average diameter of austenite grains in the structure of the tested steel was calculated by the intersection method according to PN-EN ISO 643. Whereas the qualitative assessment of non-metallic inclusions was carried out according to EN 10247.

SEM observations were made on longitudinal and transverse metallographic specimens taken from sheets of AISI 304 steel after cold rolling with a draft of 20%, using magnification up to 15000x. Observations of the microstructure were made using a scanning microscope type SUPRA<sup>TM</sup>35 from Zeiss (Germany).

TEM observations were carried out using thin foils on the samples of strip after cold-rolling with a draft of 50%. The preparation of the foils comprised a cutting out of disks, 3 mm in diameter, from a strip with a thickness of 1.0 and 0.6 mm, grinding with abrasive paper until the samples have reached a thickness of 0.1 mm.

The Tenupol-5 double jet electropolisher was used for thin foil preparation from the samples in an electrolyte containing nitric acid and methanol (1:3). The microstructure was observed by means of TEM of the

type Technai G2 F20 applying an accelerating voltage of 200kV equipped with HAADF and EDS detector. The phases were identified basing on electron diffraction. The procedure was aided by the computer software Gatan and crystallographic data base (ICDD, 2022).

X-ray qualitative and quantitative analysis of cold rolled AISI 304 steel were done by means of an X-ray diffractometer type X'PERT PANalytical, applying the filter radiation of an anode  $\lambda\text{CuK}\alpha$  (length was 0.1541 nm). The data of the diffraction lines were recorded by "step-scanning" method in  $2\Theta$  range from  $40^\circ$  to  $100^\circ$  and the  $0.05^\circ$  step, the time of measurements amounting to 10s. X-ray quantitative analysis were carried out on samples with dimensions  $10 \times 20$  mm cut from AISI 304 steel in the as-delivered condition, after supersaturation and after cold rolling with a draft from 10% to 50%. Samples for examinations were polished as well as chemical etched in  $\text{Mi17Fe}$  reagent.

### 3. RESULTS AND DISCUSSION

Metallographic observations on light microscopy were carried out to determine the effect of the degree of plastic deformation of the studied AISI 304 steel sheets during the cold rolling process. In addition, the size and shape of the primary austenite grains after supersaturation and their changes in subsequent rolling cycles as well as the effects of the plastic deformation induced martensitic transformation  $\gamma \rightarrow \alpha'$ . The degree of contamination with non-metallic inclusions was also determined in the tested steel.

In order to better characterize the phase stability of AISI 304 steel, its temperature of  $M_s$ ,  $M_{d30}$  and SFE value using empirical relations (1), (3) and (4) were calculated (Table 2).

The value of SFE for AISI 304 steel (Table 2) is very low indicating a weak stability of austenite phase in this steel. This is in agreement with the findings of Abreu (Abreu et al., 2007) and Kowalska (Kowalska et al., 2008). Moreover, the lower austenite stability in AISI 304 steel suggests in this case that the dominant mechanism of martensitic transformation is the direct  $\gamma \rightarrow \alpha'$  (Rousseau and Blanc, 1970). This paper further reports that in steels exhibiting high  $M_s$  and  $M_{d30}$  temperatures and thus low austenite stability, the  $\gamma \rightarrow \alpha'$  transformation dominates, whereas in steels with high stability (low – subzero -  $M_s$  and  $M_{d30}$  temperatures), the  $\gamma \rightarrow \epsilon \rightarrow \alpha'$  transformation prevails. In investigated AISI 304 steel both values of  $M_s$  and  $M_{d30}$  are above the zero.

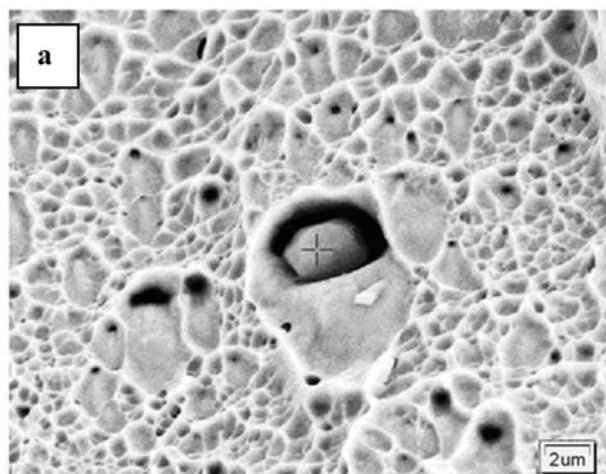
Analysis of the  $M_d$  values, temperature that 50% of austenite is transformed to martensite with 30% of deformation, suggest that the formation of martensite at room temperature for investigated AISI 304 steel is relatively easy.

Steels that present higher values of  $M_{d30}$ , for example

AISI 301 and AISI 304, are more susceptible to form induced martensite when deformed at room temperature. Steels like AISI 316 or AISI 321, that present low values for temperature  $M_{d30}$ , generally do not present strong martensite formation when deformed at room temperature (Padilha and Rios, 2002).

On the basis of the results of metallographic observations of non-etched samples, it was found that non-metallic inclusions, mainly Al and Ti oxides (standard 1a) and Ti nitrides (standard 1b and 1c, respectively), occur in the tested AISI 304 steel (PN-EN 10247). The obtained results indicate that the AISI 304 steel is characterized by high metallurgical purity. Few non-metallic inclusions are present in the tested steel and their distribution is point-like. X-ray microanalysis performed on the fractures of AISI 304 steel in the SEM (Fig. 4a), revealed inclusions of Al and Ti oxides and matrix elements (Cr and Fe, Fig. 4b). A characteristic morphological feature of the revealed non-metallic inclusions are regular polyhedral solids of the size of 2-3  $\mu\text{m}$ , located mainly at the bottom of craters and hollows of the ductile fracture surface. Moreover, spherical oxide inclusions of various sizes were also found in the investigated AISI 304 steel. The obtained structure results are consistent with literature data (Rudnik and Mazur, 1973).

The tested AISI 304 steel in the as-delivered condition shows an austenitic structure with numerous annealing twins and single inclusions. The equiaxial  $\gamma$ -solution grains have an average diameter of about 22  $\mu\text{m}$  and are characterized by a microhardness of 162HV0.05 (Fig. 5). In the supersaturated state at  $1100^\circ\text{C}$  the investigated AISI 304 steel display a single-phase austenite structure with a diameter of the average grains in the matrix  $\gamma$  amounting to about 76  $\mu\text{m}$  and a hardness of about 128 HV0.05, containing many annealed twins and single clusters of non-metallic inclusions.



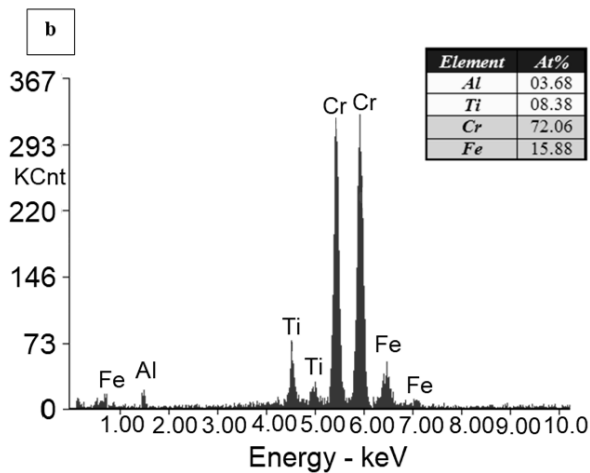


Fig 4. a) Non-metallic inclusion in the form of Ti oxides in AISI 304 steel; b) microanalysis of the inclusion

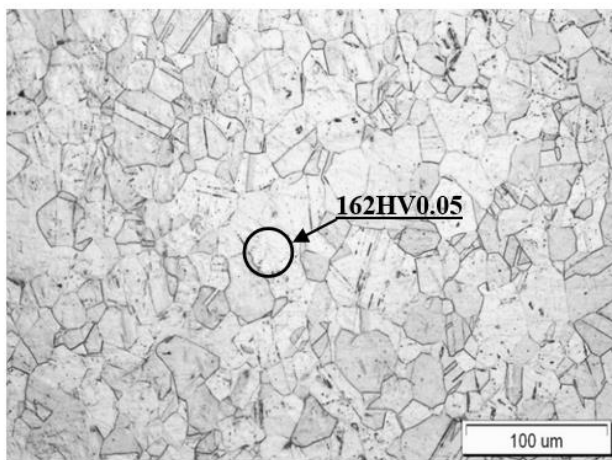


Fig. 5. Microstructure of AISI 304 stainless steel showing austenitic (fcc) structure in the as-received condition, Etching- Mi17Fe

After cold rolling with a draft of 10%,  $\gamma$  grains with strain twins and few areas of slip bands were revealed in the structure of AISI 304 steel (Fig. 6). Solution  $\gamma$  grains with slightly revealed relief and trace deformation effects inside the grains were also observed.



Fig. 6. Microstructure of AISI 304 stainless steel after 10% of deformation, Etching- Mi17Fe

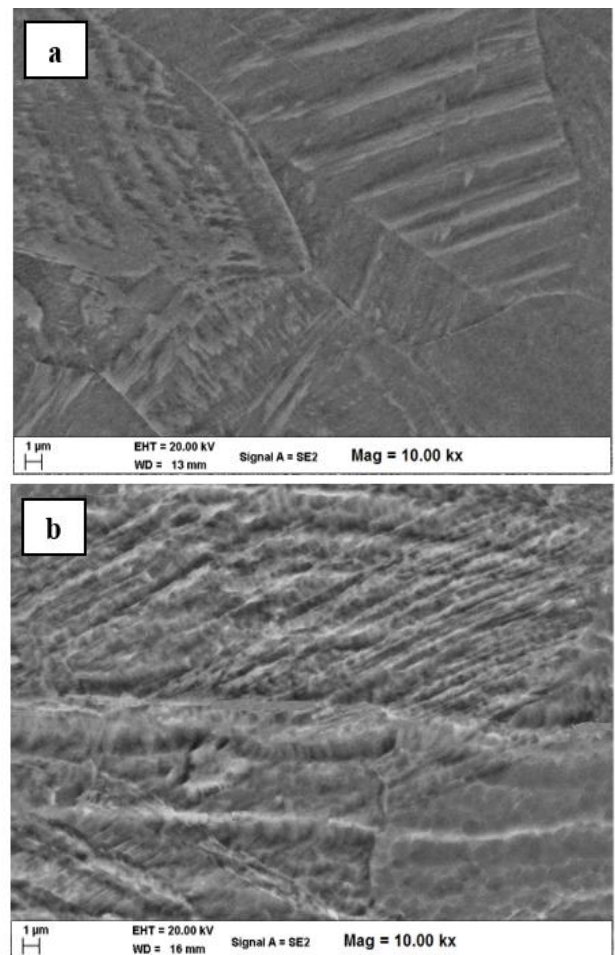


Fig. 7. Microstructure of AISI 304 stainless steel after 20% of deformation, where: a) sheet surface, deformation twins with traces of  $\alpha'$  phase; b) longitudinal section, deformation bands with  $\alpha'$  areas; Etching - Mi17Fe

The structure of the AISI 304 steel studied after cold rolling in the range from 20% to 30% is characterized by the occurrence of distinct strain bands against the background of austenite grains elongated in the direction of plastic processing (Fig.7a). Deformation effects were also observed in the form of fine parallel and intersected lines and slip bands, as well as shear bands, which are probably sites of martensite- $\alpha'$  nucleation (Fig.7b).

At a higher degree of plastic deformation (40%), the microstructure of the tested AISI 304 steel shows large areas of clearly elongated austenite grains with intersecting lines and slip bands, as well as  $\alpha'$  phase in the form of fine parallel lines. In moreover, after cold rolling with a 50% of degree of deformation a band structure with distinctly undulating strain bands located in line with the rolling direction is observed in the investigated steel (Fig 8).

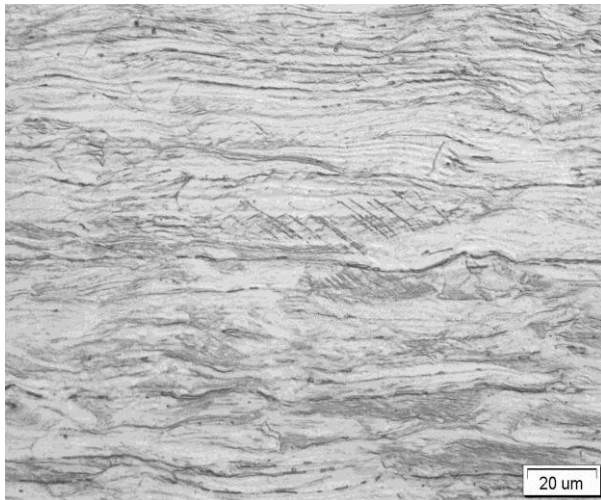


Fig. 8. Microstructure of AISI 304 stainless steel after 50% of deformation, Etching- Mi17Fe

The results of the transmission electron microscope (TEM) examination of the thin foils allowed to the analysis of the structure obtained in the AISI 304 steel under study during the cold rolling process and the  $\gamma \rightarrow \alpha'$  phase transformation induced by this process. The effect of plastic deformation in the cold rolling process was limited to the analysis of steels after 50% of degree of deformation (Fig.9 to Fig.12).

Observations in TEM also allowed to determine the morphology of phase components ( $\gamma$  and  $\alpha'$ ) and carbide precipitates of  $M_7C_3$  and  $M_{23}C_6$  types (Fig.12). Observations of thin foils of AISI 304 steel after cold rolling with a degree of deformation of 50% revealed a cellular dislocation structure of an austenitic matrix with a high dislocation density with local stacking faults, twins, carbides and  $\alpha'$  phase (Fig.9 to Fig.12).

In the microstructure of investigated AISI 304 steel the occurred of flattened and strongly elongated subgrains of austenite matrix and shearing bands dominate, and also ultra-fine lath of martensite- $\alpha'$  with a characteristic dislocation forest (Fig.10a).

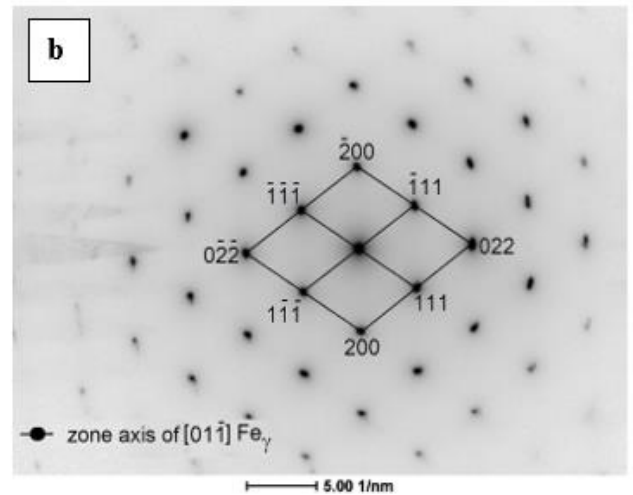
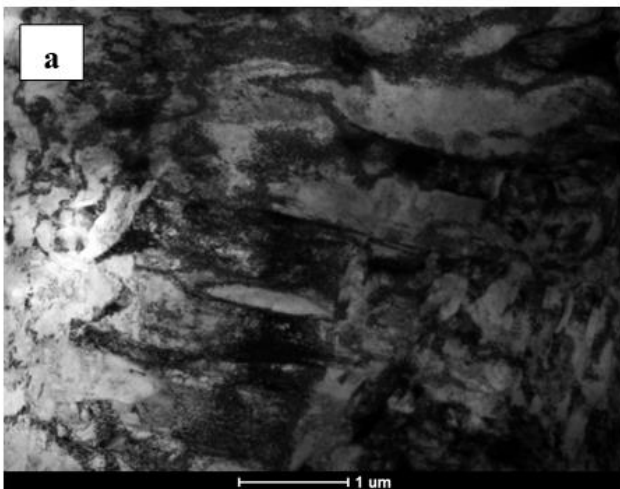
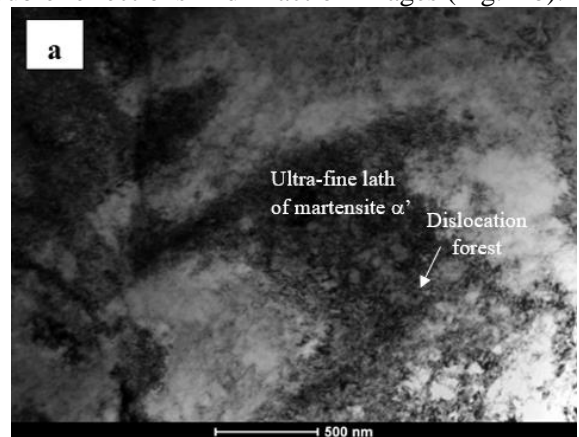


Fig. 9. a) TEM micrograph structure of AISI 304 steel after 50% of deformation, b) diffraction pattern

The Fig. 10b. shows the martensite- $\alpha'$  in the zone axis of  $[-110]$ . During the TEM examination of the thin foils of AISI 304 steel a single reflexes of the type  $(112)\alpha'$  and  $(123)\alpha'$  have been observed resulting from the martensitic phase  $\alpha'$ . According to the study (Olson and Cohen, 1975; Maxwell et al., 1974) the well known places of strain induced martensite- $\alpha'$  formation site in austenitic stainless steels are the shear bands intersection, an isolated shear band, shear band - grain boundary intersection and grain boundary triple points. In cases of investigated AISI 304 steel it may be assumed that the nucleation of phase- $\alpha'$  occurs preferentially in microtwins areas, mainly at their borders. As suggested of the study (Lee and Lin, 2000) it can be significantly associated with accumulation of the stress in a dislocations field.

In the microstructure of the AISI 304 steel also identified the occurrence of distinct mechanical twins (deformation twins) in the form of single twin crystals (Fig.11a) or in bands of micro-twins with characteristically linearly distributed, often fuzzy, double reflections in diffraction images (Fig.11b).



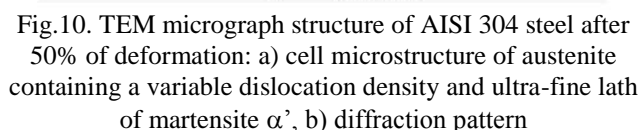


Figure 13 shows X-ray diffractograms for samples of AISI 304 steel in delivery and supersaturation state and after cold rolling with a degree of deformation from 10% to 50%. On diffraction patterns of investigated AISI 304 steel in the delivered state disclosed diffraction lines coming from planes (111), (200), (220) and (311) austenite phases, that confirmed its homogeneous  $\gamma$  structure. On diffractogram of steel after supersaturation no peaks from phase  $\alpha'$  was observed.

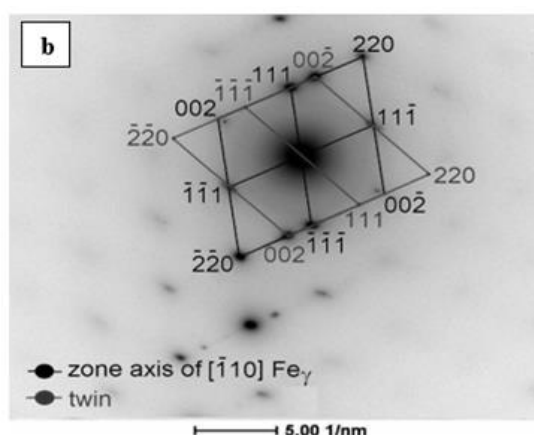
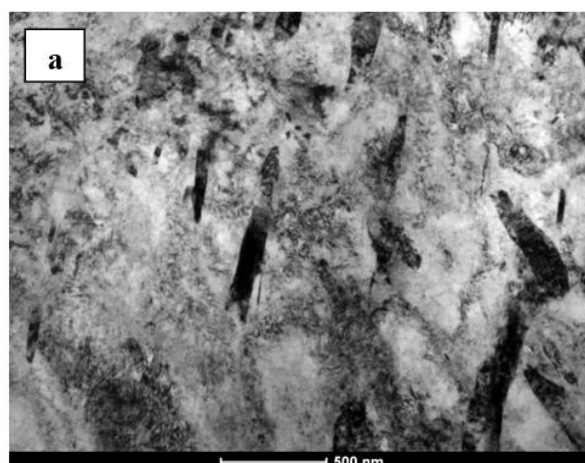


Fig. 11. TEM micrograph of AISI 304 steel after 50% of deformation: a) a band of austenite containing microtwins, b) diffraction pattern

X-ray investigations of AISI 304 steel deformed with a draft of 20% also confirmed the occurrence of  $\alpha'$  martensite in its structure.  $\alpha'$  phases were detected on diffraction patterns on the basis of the diffraction lines according to identifications from  $(110)\alpha'$  and  $(211)\alpha'$  reflection planes, which occurred with matrix lines  $\gamma$  from  $(111)\gamma$ ,  $(200)\gamma$ ,  $(220)\gamma$  and  $(311)\gamma$  reflection planes (Fig.13). After cold rolling of steel with a draft of 30%, 40%, and 50% the intensity of austenite peaks gradually decreased and martensite  $\alpha'$  peaks appeared in the spectrums. These spectra show a higher thickness reduction in the case of more numbers and a higher intensity of martensite  $\alpha'$  peaks. It was also found that with the increase of deformation the share of the reflection lines  $(110)\alpha'$  in the dual line with the reflection lines  $(111)\gamma$  increases, too. It proves a distinct increase of  $\alpha'$  phase in the structure of the investigated steel. On diffractograms only phases  $\gamma$  and  $\alpha'$  were disclosed.



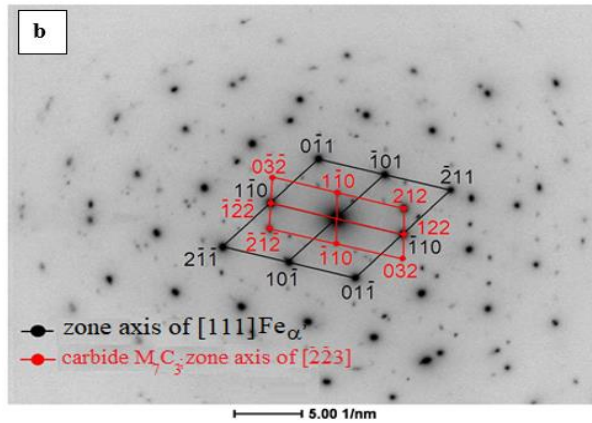


Fig.12. TEM micrograph structure of AISI 304 steel after 50% of deformation: a) dislocation structure of  $\gamma$  matrix with deformed martensite- $\alpha'$  and carbides  $M_7C_3$ , b) diffraction pattern

On the X-ray diffraction analysis of AISI 304 steel only phases  $\gamma$  and  $\alpha'$  were disclosed. There is no peak indicating the presence of  $\epsilon$  martensite. That is accordance with study of authors (Kumar et al., 2006), that have been working on cold rolled AISI304 stainless steel and also did not detected the presence of  $\epsilon$  martensite. Some other researches (Gey et al. 2005; Humbert et al. 2007) characterized deformed AISI 304 samples and detected the presence of  $\epsilon$  martensite. They have used a different apparatus. The transformation was performed in a sub-zero tension test with small deformations. It was showed that  $\epsilon$  martensite is only a step of the transformation. Increasing deformation, it transforms to  $\alpha'$ -martensite. Probably, for the amount of deformation applied in this works, the reaction  $\gamma \rightarrow \epsilon \rightarrow \alpha'$  has been completed. The martensitic transformation is important for the mechanical properties. The martensite- $\alpha'$  is generally the main transformation phase, but also the martensite  $\epsilon$  is believed to have an impact. The martensite is harder and stronger than the austenite. Hence, the metastable stainless steels have a high strain hardening upon deformation, both due to the increased dislocation density and the composite strengthening generated by the martensite (Angel, 1954; Hedström et al., 2007).

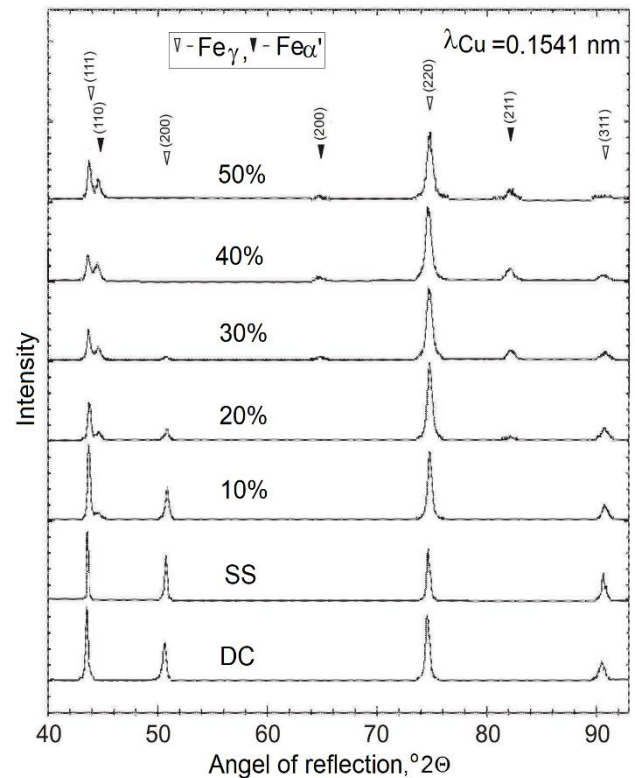


Fig. 13. X-ray diffraction patterns of steel AISI 304 in delivery condition (DC), supersaturation state (SS) and deformed state with a draft from 10% to 50%

The occurrence of  $\alpha'$  martensite in the structure of the studied AISI 304 steel was confirmed by X-ray analysis results, as well as by mechanical properties and hardness measurements. The values of tensile strength UTS, yield point  $YS_{0.2}$  and hardness HV5 were found to increase with increasing degree of deformation, while the value of elongation  $EL_{75}$  decreased (Fig. 14).

In the supersaturated state, the mechanical property indices of the tested AISI 304 steel are respectively: UTS=595MPa,  $YS_{0.2}$ =260MPa and  $EL_{75}$ =61%, and the hardness is equal to 146 HV5. The plastic deformation of AISI 304 steel sheets in the process of cold rolling with a range from 10% to 50% causes a significant increase in UTS from about 785 MPa to about 1258 MPa,  $YS_{0.2}$  from about 586 to about 1060 MPa (Fig.14). The plastic properties of the investigated steel in the analysed range of deformation, determined on the basis of  $EL_{75}$ , decrease from about 32% to about 1.1% (Fig.14). On the other hand, the hardness of the investigated AISI 304 steel after cold rolling increases monotonically with increasing of degree of deformation from 10% to 50%, and in the analyzed strain range it increases from about 260 HV5 to the maximum value of about 410 HV5 (Fig. 14).

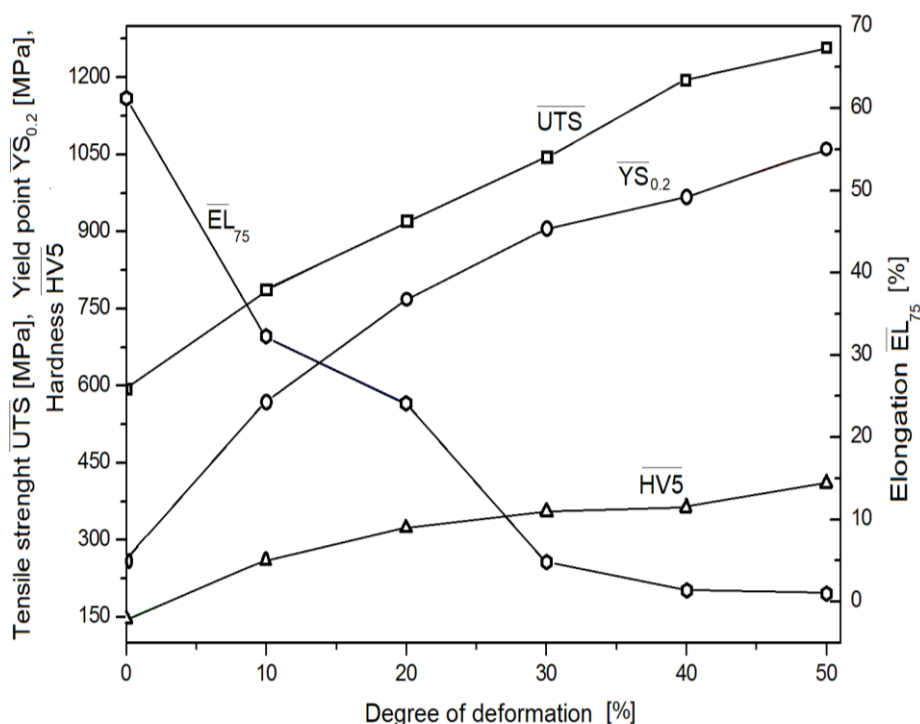


Fig. 14. Effect of the degree of deformation on mechanical properties and hardness of cold-rolled AISI 304 steel

#### 4. CONCLUSIONS

Plastic deformation of metals of A1 (fcc) lattice, including corrosion-resistant steels of austenitic structure, which occur during cold deformation in the process of e.g. rolling, drawing or deep pressing, causes not only a significant change of their physical and mechanical properties, but also brings the structural changes. These changes are revealed primarily by an increase in hardness and strength with a simultaneous decrease in plastic properties and a decrease in electrical conductivity and density, as well as by the formation of the deformation texture (Abreu, 2007), which significantly affects the occurrence of anisotropic properties of A1 lattice metals. The mechanical properties results showed that with increasing of the degree of plastic deformation in the cold rolling process of AISI 304 steel sheets, in the range from 10% to 50%, causes pronounced changes in the structure of the steel, namely: an increase in the proportion of elongated (flattened) grains of the  $\gamma$  matrix and the  $\alpha'$  phase, an increase in slip lines and strain and shear bands, as well as mechanical twins, which determine a significant increase in their strength properties and a decrease in their plastic properties. In particular, the yield strength ( $YS_{0.2}$ ) from ca. 586 to ca. 1060 MPa in the studied steel, and the steel tensile strength (UTS) from ca. 785 MPa to ca. 1258 MPa. On the other hand, the plastic properties determined by elongation ( $EL_{75}$ ), decrease from ca. 32% to ca. 1%.

A strong effect of plastic deformation is found to be

the strain hardening of the investigated AISI 304 steel. The hardness of the AISI 304 steel after cold rolling increases monotonically with increasing of degree of deformation from 10% to 50%, and in the analyzed strain range it increases from about 260 HV5 to the maximum value of about 410 HV5.

The TEM results showed that under high degree of deformation, ca. 50% the microstructure of the investigated AISI 304 steel displays a high dislocation density in the matrix  $\gamma$  and the presence of mechanical twins, as well as shearing bands in area where the lamellar formations of martensite- $\alpha'$  phase nucleate. TEM results also showed that martensite nucleates at more than one location, i.e.: shear band intersection, isolated shear band and microtwins. In cases of investigated AISI 304 steel it may be assumed that the nucleation of phase- $\alpha'$  occurs mostly preferentially in microtwins areas, mainly at their borders. Accordingly, direct martensitic transformation mechanism, viz.  $\gamma(\text{fcc}) \rightarrow \alpha'(\text{bcc})$  have been observed during deformation of AISI 304 stainless steel within in whole range of applied strain. The X-ray investigations of cold-rolled AISI 304 steel confirmed the occurrence of martensite- $\alpha'$  in the steel structure.  $\alpha'$  phases were detected on diffraction patterns on the basis of the diffraction lines according to identifications from  $(110)\alpha'$  and  $(211)\alpha'$  reflection planes, which occurred with matrix lines  $\gamma$  from  $(111)\gamma$ ,  $(200)\gamma$  and  $(220)\gamma$  reflection planes.

## 5. REFERENCES

1. Abreu, H., Carvalho, S., Neto, P., Santos, R., Freire V., Silva, P., Tavares, S., (2007). *Deformation induced martensite in an AISI 301LN stainless steel: Characterization and influence on pitting corrosion resistance*, Mater. Res., 10(4), 359-366.
2. Ahlers, M., (2004). *The martensitic transformation*, Rev. Mater., 9, 169-183.
3. Amar, K., Murdock, D.C., Mataya, M.C., Speer, J.G., Matlock, D.K., (2004). *Quantitative measurement of deformation-induced martensite in 304 stainless steel by X-ray diffraction*, Scr. Mater., 50, 1445-1449.
4. Angel, T., (1954). *Formation of martensite in austenitic stainless steels: Effects of deformation, temperature and composition*, J. Iron Steel Inst., 177, 165-174.
5. Bavay, J.C., (1993). *Les aciers inoxydables austénitiques*, Journal de physique; (France), 5, 562-570.
6. Blicharski, M., Gorczyca, S., (1978). *Structural inhomogeneity of deformed austenitic stainless steel*, Met. Sci. J., 12(7), 303-312.
7. Cina B., (1958). *A transitional h.c.p. phase in the  $\gamma \rightarrow \alpha$  transformation in certain Fe-Base alloys*, Acta Metall., 6(12), 748-762.
8. Dai, Q.X., Cheng, X.N., Zhao, Y.T., Luo, X.M., Yuan, Z.Z., (2004). *Design of martensite transformation temperature by calculation for austenitic steels*, Mater. Charact., 52(4-5), 349-354.
9. Das, A., Sivaprasad, S., Ghosh, M., Chakraborti, P.C., Tarafder, S., (2008). *Morphologies and characteristics of deformation induced martensite during tensile deformation of 304LN stainless steel*, Mat. Sci. and Eng., 486A, pp.283-286. 37.
10. Gey, N., Petit, B., Humbert M., (2005). *Electron backscattered diffraction study of  $\epsilon/\alpha'$  martensitic variants induced by plastic deformation in 304 stainless steel*, Metall. Mater. Trans., 36A, pp. 3291-3299.
11. Hedström, P., Lienert, U., Almer, J., Odén, M., (2007). *Stepwise transformation behaviour of the strain-induced martensitic transformation in a metastable stainless steel*, Scr. Mater., 55, 213-216.
12. Humbert, M., Petit, B., Bolle, B., Gey, N., (2007). *Analysis of the  $\gamma \rightarrow \epsilon \rightarrow \alpha'$  variant selection induced by 10% plastic deformation in 304 stainless steel at -60°C*, Mater. Sci. Eng., 454-455A, 865-867.
13. Kowalska, J., Ratuszek, W., Chruściel, K., (2008). *Crystallographic relations between deformation and annealing texture in ed AISI austenitic steels*, Arch. Metall. Mater., 53(1), 125-130.
14. Kumar, B.R., Singh, A.K., Mahato, B., De, P.K., Bandyopadhyay, N.R., Bhattacharya, D.K., (2006). *Induced transformation textures in metastable austenitic stainless steel*, Mater. Sci. Eng., 429A, 205-211.
15. Kurc-Lisiecka, A., Ozigowicz, W., Kalinowska-Ozigowicz, E., Maziarz, W., (2016). *The microstructure of metastable austenite in X5CrNi18-10 steel after its strain - induced martensitic transformation*, Mater. Techn., 50 (6), 837-843.
16. Lagneborg, R., (1964). *The martensite transformation in 18%Cr-8%Ni steels*, Acta Metall., 12, 823-843.
17. Leber, H.J., Niffenegger, M., Kalkhof, D., (2004). *Determination of deformation-induced martensite in austenitic stainless steel*, Proc 4<sup>th</sup> Int Conf on NDE in Relation to Structural Integrity for Nuclear and Pressurized Components. London, pp.6-8.
18. Lee, W.S., Lin, C.F., (2000). *The morphologies and characteristics of impact-induced martensite in 304L stainless steel*, Scr. Mater., 43(8), 777-782.
19. Lo, K.H., Shek, C.H., Lai, J.K.L., (2009). *Recent development in stainless steels*, Mat. Sci. and Eng. R, 65, 39-104.
20. Maxwell, P.C., Goldberg, A., Shyne, J.C., (1974). *Stress-assisted and Strain-induced martensites in Fe-Ni-C Alloys*, Metall. Trans., 5, pp.1305.
21. Murr, L.E., (1981), *Shock Waves and High-Strain-Rate Phenomena in Metals* in: Concepts and Applications, editor M.A., Meyers, L.E., Murr, eds., Plenum Press, New York, NY, pp. 607-73.
22. Olson, G.B., Cohen, M., (1972). *A mechanism for the strain-induced nucleation of martensitic transformations*, Journal of the Less-Common Metals, 28, 107-118.
23. Olson, G.B., Cohen, M., (1975). *Kinetics of strain-induced martensitic nucleation*, Metall. Trans. 6A, 791-799.
24. Padilha, A.F., Rios, P.R., (2002). *Decomposition of austenite in austenitic stainless steel*, ISIJ International, 42(4), 325-337.
25. Padilha, A.F., Plaut, R.L., Rios, P.R., (2003). *Annealing of cold-worked austenitic stainless steels*, ISIJ International, 43(2), 135-143.
26. Pater, Z., (2014). *Fundamentals of metallurgy and foundry engineering*. Lublin University of Technology Publishing House, pp.38-40.
27. Powder Diffraction File for International Center for Diffraction Data (ICDD, 2022). Available from <https://www.icdd.com/pdfsearch/>, Accessed: 2/4/2022.
28. Reed, R., (1962). *The spontaneous martensitic transformations in 18%Cr, 8%Ni steels*, Acta Metall., 10, 865-877.
29. Rousseau, D., Blanc, G., (1970). *Stabilité structurale à la déformation et au froid des aciers inoxydables austénitiques au Cr-Ni*, Mém. Etud. Sci. Rev. Metall., 67(5), 315-334.
30. Rudnik, S., Mazur, W., (1973). *Inclusions in austenitic stainless steel*, Metallurgist, 4, 162-169.
31. Schramm, R.E., Reed, R.P., (1975). *Stacking fault energies of Austenitic Stainless Steels*, Metall. Trans. A, 6A, 1345-1351.
32. Shin, H.C., Ha, T.K., Chang, Y.W., (2001). *Kinetics of deformation induced martensitic transformation in 304 stainless steel*, Scr. Mater., 45,

823-829.

33. Shrinivas, V., Varma, S.K., Murr, L.E., (1995). *Deformation-induced martensitic characteristics in 304 and 316 stainless steels during room-temperature rolling*, Metall. Mater. Trans. A, 26(3), 661-671.

34. Standard PN-EN ISO 6892-1: *Metallic Materials - Tensile Testing - Part 1: Method of test at room temperature*.

35. Standard PN- EN ISO 6507-1: *Metallic materials – Vickers hardness test - Part 1: Test method*.

36. Standard PN-EN ISO 643: *Steels – Micrographic determination of the apparent grain size*.

37. Standard PN-EN 10247: *Micrographic examination of the non-metallic inclusion content of steels using standard pictures*.

38. *Standard Practice for Microetching Metals and Alloys* - ASTM E407.

39. Venables, J.A., (1962). *The martensite transformation in stainless steel*, Philos. Mag. Lett., 73, 35-44.